Available online at www.sciencedirect.com
SCIENCE DIRECT
Carbohydrate Research 341 (2006) 1834–1847
Carbohydrate RESEARCH

# Structural characterization of underivatized arabino-xylo-oligosaccharides by negative-ion electrospray mass spectrometry

Bernard Quéméner,* José Juan Ordaz-Ortiz and Luc Saulnier

*INRA—Biopolymères, Interactions, Assemblages—Rue de la Géraudière BP 71627, F-44316 Nantes, France*

Received 29 December 2005; received in revised form 20 April 2006; accepted 22 April 2006
Available online 30 May 2006

**Abstract**—Various arabino-xylo-oligosaccharides with known substitution patterns were assessed by negative ESI-Q-TOFMS and ESI-ITMS. The CID spectra of linear xylo-oligosaccharides and of nine isomeric mono- and disubstituted arabino-xylo-oligosaccharides established that structures differing in their substitution pattern can be differentiated by this approach. The negative-ion fragmentation spectra of the deprotonated quasi-molecular ions are mainly characterized by glycosidic cleavage ions from the C-series, which provide sequence informations, and by cross-ring cleavage $^{0,2}A_i$ ions, which provide partial linkage information. When the collision energy increased, the cross-ring cleavage $^{0,2}A_i$ ions underwent consecutive loss of water to produce $^{0,2}A_i - 18$ fragment ions and glycosidic cleavage ions of the B-series are also produced besides the $C_i$ ions. Contrary to linear xylo-oligosaccharides, $C_i$ ions, which originate from C-3 monosubstituted xylosyl residues never produce the related cross-ring cleavage $^{0,2}A_i$ ions. Disubstitution at O-2 and O-3 of xylosyl residues appears to enhance the production of the $^{0,2}A_i$ ions compared to monosubstitution. For the differentiation of the mono- and disubstitution patterns of the penultimate xylosyl residue, the relative abundance of the glycosidic cleavage ions at $m/z$ 263 and 299 found on Q-TOF CID spectra plays a relevant role and appears to be more informative than $MS^n$ spectra obtained on a ion trap instrument.


*Keywords:* Oligosaccharides; Structural isomers; Xylanase; ESI-Q-TOFMS; ESI-ITMS

## 1. Introduction

Arabinoxylans (AX) are the main non-starch polysaccharides from wheat grain cell walls. They consist of a linear backbone of β-(1→4)-linked D-xylopyranosyl residues. Xylosyl units can be unsubstituted, monosubstituted at C-3 or disubstituted at C-2 and C-3 with α-L-arabinofuranosyl units.[1] In wheat endosperm, AX are partly water-extractable (25%, WE-AX) and exhibit an average arabinose to xylose ratio (A/X) of 0.6. Natural variations in the structure of WE-AX (A/X) ratio have been described. The structure of water unextractable AX (WU-AX), which represent the major part of AX in the cell walls of endosperms is essentially the same but a higher A/X ratio has been reported.[2,3] Variation in the degree of branching and in the spatial distribution of arabinosyl substituents along the xylan backbone is responsible for the biological and physicochemical properties.[1] The structure of arabinoxylans has been investigated in the past decade using $^1H$ and $^{13}C$ NMR spectroscopy, and numerous studies have been reported on the structural characterization of oligosaccharides obtained after xylanase digestion of AX.[1,4–11] Although, NMR sensitivity has considerably improved with the introduction of nanoprobe equipments and very high field magnets, this approach still requires large amounts of high purity samples.[12,13]

As an alternative to NMR spectroscopy, FABMS and ESIMS have been used for oligosaccharide characterization. The main advantages of ESIMS are its sensitivity, and capability to assign linkage,[14–18] sequence and

* Corresponding author. Tel.: +33 2 40 67 50 65; e-mail addresses: bernard.quemener@nantes.inra.fr; quemener@nantes.inra.fr

0008-6215/$ - see front matter © 2006 Elsevier Ltd. All rights reserved.
doi:10.1016/j.carres.2006.04.039

branching[19,20] or substituent pattern[21–26] informations upon collision-induced dissociation (CID) of underivatized oligosaccharides. Moreover, derivatization, for example, permethylation[27–29] or reducing-end derivatization[30–34] in combination with CID[35–39] proved to be very useful to clearly identify complex branching patterns of oligosaccharides. Recently, the characterization of a complex oligosaccharides mixture obtained by enzymatic digestion of AX from wheat seeds was carried out using MALDI-TOFMS and ESI-Q-TOFMS or ESI-ITMS.[40] Underivatized linear and branched structures could not be distinguished upon CID using positive-ion mode in either Q-TOF or IT instruments. Permethylation of the oligosaccharides followed by ESI-ITMS with multiple MS steps ($MS^n$) allowed to partially characterize complex xylo-oligosaccharide structures differing by the number of arabinose residues and their spatial arrangement along the xylose backbone. However, additional techniques of derivatization and GC–MS were necessary to assign the position of the Ara*f* substituent at C-3 of the Xyl*p* residue.[41] Some authors have reported that sequence and branching patterns of underivatized oligosaccharides can however be obtained using negative CID-ESIMS/MS.[18,42–45] The main advantage of negative CID MS/MS is to produce a series of C-type glycosidic cleavage ions, which produce in turn a series of related A-type cross-ring cleavage ions carrying linkage information.[14,23,44–46] In addition, specific D-ions arising from double D-type cleavage at the 3-linked glycosidic bond, may also be produced.[42,43] Recently, negative $CIDMS^n$ was successfully applied to the assignment of acetyl groups to O-2 and/or O-3 positions of pectic oligogalacturonides[24] and of the feruloyl group to O-2 or O-5 of arabinosyl residues and to O-6 of a galactosyl-containing disaccharide.[18]

ESI-ITMS and ESI-Q-TOFMS using negative-ion mode are now assessed for the structural differentiation of eight underivatized mono- and disubstituted xylo-oligosaccharides obtained from enzymatic digestion of wheat WE-AX by an endoxylanase from *Trichoderma viride*.[47] Linear, mono- and disubstituted xylo-oligosaccharides were structurally differentiated upon CID using a Q-TOF instrument in MS/MS experiments.

## 2. Results and discussion

The eight mono- and disubstituted xylo-oligosaccharides released by enzymatic degradation of wheat WE-AX by an endoxylanase from *T. viride*, were purified by size-exclusion chromatography on Biogel P2 alone or combined with semi-preparative HPAEC.[47] They generally contained less than 3–5% of visible contaminants as determined by HPAEC and ESI-Q-TOFMS. Due to the specificity of the action of the enzyme used, the oligosaccharides were obtained with identical sequences at both ends, namely one and two free xylosyl residues at the non-reducing and reducing end, respectively[47] (Chart 1). In addition monosubstitution is only found at O-3 in wheat AX. Consequently, $A1_2X3$, $A1_3X4$, $A2_{3d}X4$ and $A2_{4,3}X5$ are single isomers for DP 4, DP 5, DP 6 and DP 7, respectively. $A2_{4,3}X5$ (DP 7) and $A2_{5,3}X6$ (DP 8), which co-eluted in the conditions of analytical HPAEC, were separated in conditions used for the semi-preparative HPAEC.[47] Anyway, in this specific case, it was easy to select the appropriate ion, on a mass basis, for tandem mass spectrometry as the relevant $m/z$ for these two oligosaccharides were 941 and 1073, respectively. Fortunately, the three isomers of DP 8 were well separated by HPAEC (retention times 21.0; 23.3 and 24.3 min for $A2_{5,3}X6$, $A3_{4,3d}X5$ and $A3_{4d,3}X5$, respectively).

To establish the main fragmentation patterns of oligosaccharides through CID experiment, $^{18}O$-labelling was carried out at the reducing end. This allowed to discriminate isobaric ions, especially $B_i$ from $Z_j$ ions and $C_i$ from $Y_j$ ions, according to the nomenclature of Domon and Costello.[48] Only $Z_j$ and $Y_j$ ions, which contain the reducing end, are $^{18}O$-labelled and are characterized by a mass increment of 2 Da. Prior analysis performed by negative ESI-ITMS with multiple MS steps revealed to be more time consuming, less sensitive and less informative than ESI-Q-TOFMS regarding the arabinosyl residues distribution along the xylopyranosyl backbone, particularly for oligomers of DP 6 and more. Therefore, most of the results presented in the following section were obtained using ESI-Q-TOFMS. But generally, the main diagnostic fragment ions were also produced using $ESI\text{-}ITMS^n$.

### 2.1. General features of negative ESI-Q-TOF tandem mass spectrometry of AX and linear xylo-oligosaccharides

The complete MS spectra of linear xylo-oligosaccharides and of AX were generally dominated by the singly charged $[M^*-H]^-$ and $[M^*-H+36]^-$ quasi-molecular ions. The +36 additional mass was attributed to the solvatation of the molecule by two molecules of water. Indeed, MS/MS experiment performed on the $[M^*-H+36]^-$ quasi-molecular ion showed the $[M^*-H]^-$ species as the main daughter ion besides the same glycosidic cleavage ions as produced upon direct fragmentation of the $[M^*-H]^-$ quasi-molecular ion. However, the collision energy necessary to obtain roughly similar $MS^2$ spectra was in all cases much higher with the dihydrated molecule. In order to obtain a maximum amount of the precursor ions, the first-order spectra were obtained using low collision energy (10 eV). Under these conditions, some fragment ions such as the ion at $m/z$ 299, which may be considered as diagnostic ions in the $MS^2$ spectrum, were already present on the full MS spectrum.

The collision energy needed to fragment compounds under CID conditions increases as a function of the

| Oligomers[a] | DP | Structure |
|---|---|---|
| $A1_2X3$ | 4 | 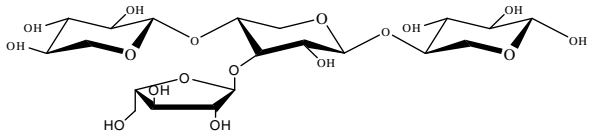 |
| $A1_3X4$ | 5 | 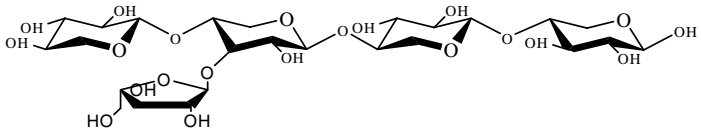 |
| $A2_{3d}X4$ | 6 | 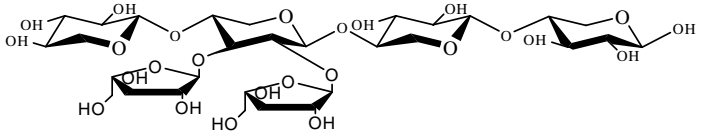 |
| $A2_{4,3}X5$ | 7 | 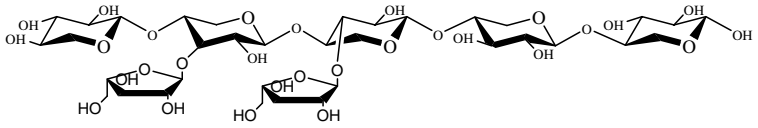 |
| $A3_{4,3d}X5$ | 8 | 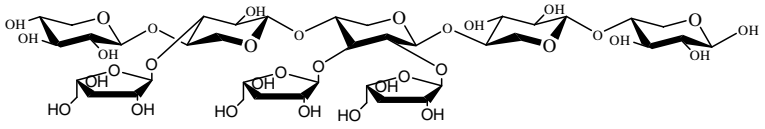 |
| $A3_{4d,3}X5$ | 8 | 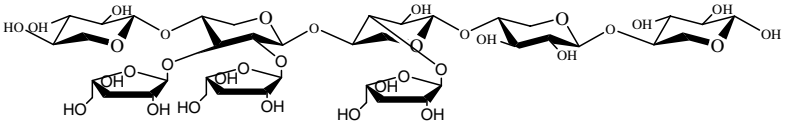 |
| $A2_{5,3}X6$ | 8 | 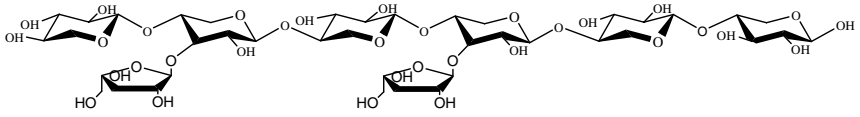 |
| $A4_{4d,3d}X5$ | 9 | 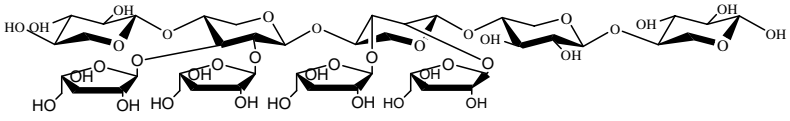 |

[a] Subscript figure is related to the position of arabinose substituents on xylo-oligosaccharides. Xylose residues are numbered from the reducing end. Letter d refers to di-substitution.

**Chart 1.** Structure of the eight branched arabino-xylo-oligosaccharides isolated from wheat AX.

molecular mass[19] (Table 1). To enhance the abundance of specific fragment ions, the collision energy was set to about zero for oligosaccharides of DP 6 and higher to reduce the precursor ion signal. The $^{18}O$-labelling allowed to infer the main direction of the fragmentation from the reducing to the non-reducing end of the molecule. Indeed, this was supported on one hand by the absence in all CID spectra of $^{18}O$-labelled glycosidic cleavage ions of the Z-series except for the $Z_1^*$ ion at $m/z$ 133 and on the other hand by the main residue lost,

**Table 1.** Collision energies required to reduce to 50% the abundance of the $[M-H]^-$ parent ion from linear xylo-oligosaccharides and branched arabino-xylosaccharides using ESI-Q-TOF in negative-ion mode and main product ions obtained with their assignment[48]

| Oligomer | Structure | Collision energy (50% parent ion fragmentation) | $[M-H]^-$ | *m/z* of main characteristic fragment ions | | | | | | | | | | | | |
|---|---|---|---|---|---|---|---|---|---|---|---|---|---|---|---|---|
| | | | 1127 | 995 | 881 | 863 | 731 | 617 | 599 | 545 | 485 | 413 | 395 | 353 | 299 | 281 | 263 | 149 |
| DP 9 | $A4_{4d,3d}X5$ | 25 | 1205 | $^{0,2}A_5-18$ | $^{0,2}A_4-18$ | | | | | n.c.[a] | | | n.c. | | | | n.c. | $C_1$ |
| DP 8 | $A3_{4d,3}X5$ | 22 | 1073 | | $^{0,2}A_5-18$ | $^{0,2}A_4-18$ | | | | n.c. | | | n.c. | | | | n.c. | $C_1$ |
| DP 8 | $A3_{4,3d}X5$ | 23 | 1073 | | $^{0,2}A_5-18$ | $^{0,2}A_4$ | | | | | | n.c. | | | $Y_{4\alpha}/C_2$ | | n.c. | $C_1$ |
| DP 8 | $A2_{5,3}X6$ | 23 | 1073 | | $^{0,2}A_6-18$ | | $^{0,2}A_5-18$ | | | $C_3$ | $^{0,2}A_3$ | n.c. | | | $Y_{5\alpha}/C_2$ | | n.c. | $C_1$ |
| DP 7 | $A2_{4,3}X5$ | 20 | 941 | | | | $^{0,2}A_5-18$ | | | n.c. | | n.c. | | | $Y_{4\alpha}/C_2$ | | n.c. | $C_1$ |
| DP 6 | $A2_{3d}X4$ | 18 | 809 | | | | | $^{0,2}A_4-18$ | $^{0,2}A_3-18$ | | | | n.c. | | | | n.c. | $C_1$ |
| X6 | X6 | 18 | 809 | | | | | $^{0,2}A_6-18$ | $^{0,2}A_5-18$ | | $^{0,2}A_4$ | | | | | $C_2$ | | $C_1-18$ |
| DP 5 | $A1_3X4$ | 15 | 677 | | | | | $^{0,2}A_4$ | | | $^{0,2}A_3$ | n.c. | | | $Y_{3\alpha}/C_2$ | | $Z_{3\alpha}/C_2$ | $C_1$ |
| X5 | X5 | 16 | 677 | | | | | $^{0,2}A_5$ | $^{0,2}A_5-18$ | $C_4$ | $^{0,2}A_4$ | $C_3$ | | $^{0,2}A_3$ | | $C_2$ | | $C_1-18$ |
| DP 4 | $A1_2X3$ | 9 | 545 | | | | | | | | | $C_2$ | | | $Y_{2\alpha}/C_2$ | | $Z_{2\alpha}/C_2$ | $C_1$ |
| X4 | X4 | 12 | 545 | | | | | | | | $^{0,2}A_4$ | $C_3$ | | $^{0,2}A_3$ | | $C_2$ | | $C_1-18$ |
| X3 | X3 | 7 | 413 | | | | | | | | | | | $^{0,2}A_3$ | | $C_2$ | | $C_1-18$ |

[a] n.c.: the fragment ion was present but 'not characterized'.

which was always the $^{18}O$-labelled reducing xylosyl residue as attested by the 134 (132 + 2) Da loss resulting in the complementary $C_{n-1}$ ion (see the ions at *m/z* 281, Figs. 1a and c). The absence of glycosidic cleavage ions resulting from a 132 Da loss from the quasi-molecular $(M^*-H)^-$ precursors ions suggests that the presence of the arabinosyl substituent did not affect the direction of fragmentation. This oriented fragmentation could be explained by the retention of the negative charge at the reducing xylosyl unit. Contrary to pectic α-(1→5)-linked arabinan chains,[49] the $[M^*-H]^-$ quasi-molecular ion from both linear xylo-oligosaccharides and AX did not undergo loss of water under CID. This difference in behaviour might be ascribable to the furanose and pyranose rings, which characterize pectic α-(1→5)-linked arabinan chains and the xylopyranosyl backbone of linear xylo-oligosaccharides or AX, respectively. More interestingly, glycosidic ions cleavage generated from the $[M^*-H]^-$ quasi-molecular ion upon fragmentation at low collision energy of both linear and branched xylo-oligosaccharides were mainly from the C-series using ESI-ITMS$^n$ or ESI-Q-TOFMS/MS (Table 1). This result indicates that under negative ionization mode the glycosidic cleavage occurred preferentially on the reducing side of the glycosidic oxygen atom.[14,18,42] Cross-ring cleavage $^{0,2}A_i$ ions, which may be considered as diagnostic ions for (1→4) linkage, were also produced from linear xylosides and from the linear part of AX. When the collision energy increased, these cross-ring cleavage $^{0,2}Ai$ ions underwent consecutive water loss to produce $^{0,2}A_i-18$ fragment ions and glycosidic cleavage ions of the B-series were also produced besides the $C_i$ ions. CID experiments carried out on the $C_2$ ion at *m/z* 281 and generated from xylotriose (Fig. 1b), allowed to ascertain from the absence of −18 mass units loss (absence of ion at *m/z* 263), that these fragment ions arised really from the B-series and not from $C_i-18$ ions. In other terms, these $B_i$ ions were produced by competitive and not consecutive dissociation. The mechanism of formation of the $^{0,2}A_i-18$ fragment ions via loss of water from the $^{0,2}A$ cross-ring cleavage ions has previously been proposed by Mulroney et al.[50] The presence of both specific fragment ions arising from cross-ring cleavages indicates that xylosyl units are (1→4)-linked.[14,42,46,50] The presence of some fragment ions due to $C_3H_6O_3$ (90 Da) loss was unexpected. These ions were present on linear and substituted xylo-oligosaccharides MS/MS spectra and may correspond to $^{0,3}A$ ion series because a loss of 92 Da was produced from the $^{18}O$-labelled $[M^*-H]$ precursor.

## 2.2. ESI-CIDMS analysis of linear xylo-oligosaccharides

The collision energy needed to fragment linear xylo-oligosaccharides was generally higher than that used for the related mono- or disubstituted oligomers, as previously

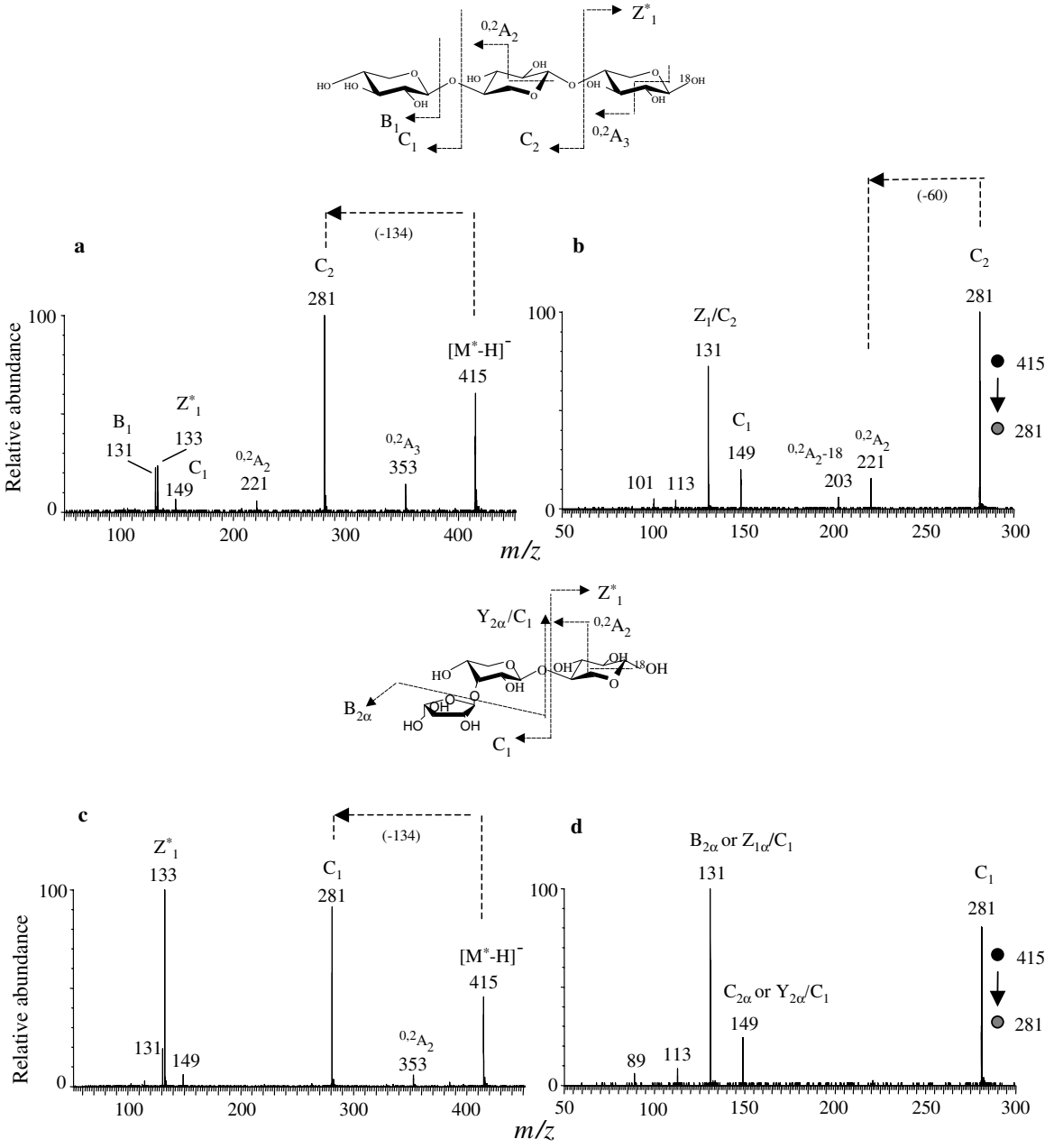


**Figure 1.** Chemical structures and CID mass spectra of the $^{18}$O-labelled $[M^*-H]^-$ quasi-molecular ion from (a) linear xylotriose, (c) $A1_2X2$ using ESI-Q-TOF at 50% fragmentation level of the $[M^*-H]^-$ precursor ion. (b) and (d) are CID mass spectra after trapping in source of the glycosidic fragment ions at *m/z* 281 from xylotriose and $A1_2X_2$, respectively. Fragments are identified according to Domon and Costello nomenclature.[48] Asterisks indicate the $^{18}$O-labelled ions.

reported in positive-ion mode.[40] Using a similar collision energy, linear xylo-oligosaccharides generally fragment more than monosubstituted AX isomers. This observation is in agreement with the previous results obtained on oligosaccharides derived from human milk using MALDI- FTMS.[38] Moreover, fragment ions yield were generally higher than those obtained in positive-ion mode on sodium adducts of xylo-oligosaccharides.[51]

Similar MS/MS fragmentation patterns were observed for all linear xylo-oligosaccharides studied (X2, X3, X4, X5 and X6). The ESI-Q-TOFMS/MS spectra of $^{18}$O-labelled X3, X4 and X5 are presented in Figures 1a, 2a and 3a. All the glycosidic cleavage $C_i$ ions dissociated according to specific cross-ring cleavage $^{0,2}$A ions due to the loss of the $C_2H_4O_2$ ring fragment (60 Da) typical of the (1→4) linkage. The $^{0,2}A_4$ ion at *m/z* 485 (Fig. 2a) and the $^{0,2}A_5$ ion at *m/z* 617 (Fig. 3a) were prominent fragment ions at 50% fragmentation level. These ions were due to the 62 Da loss related to the labelled $C_2H_4O^{18}O$ ring fragment. Surprisingly, the $B_1$ ion at *m/z* 131 on CID spectra of X4, X5 (Figs. 2a and 3a) and X6 (not shown) was more

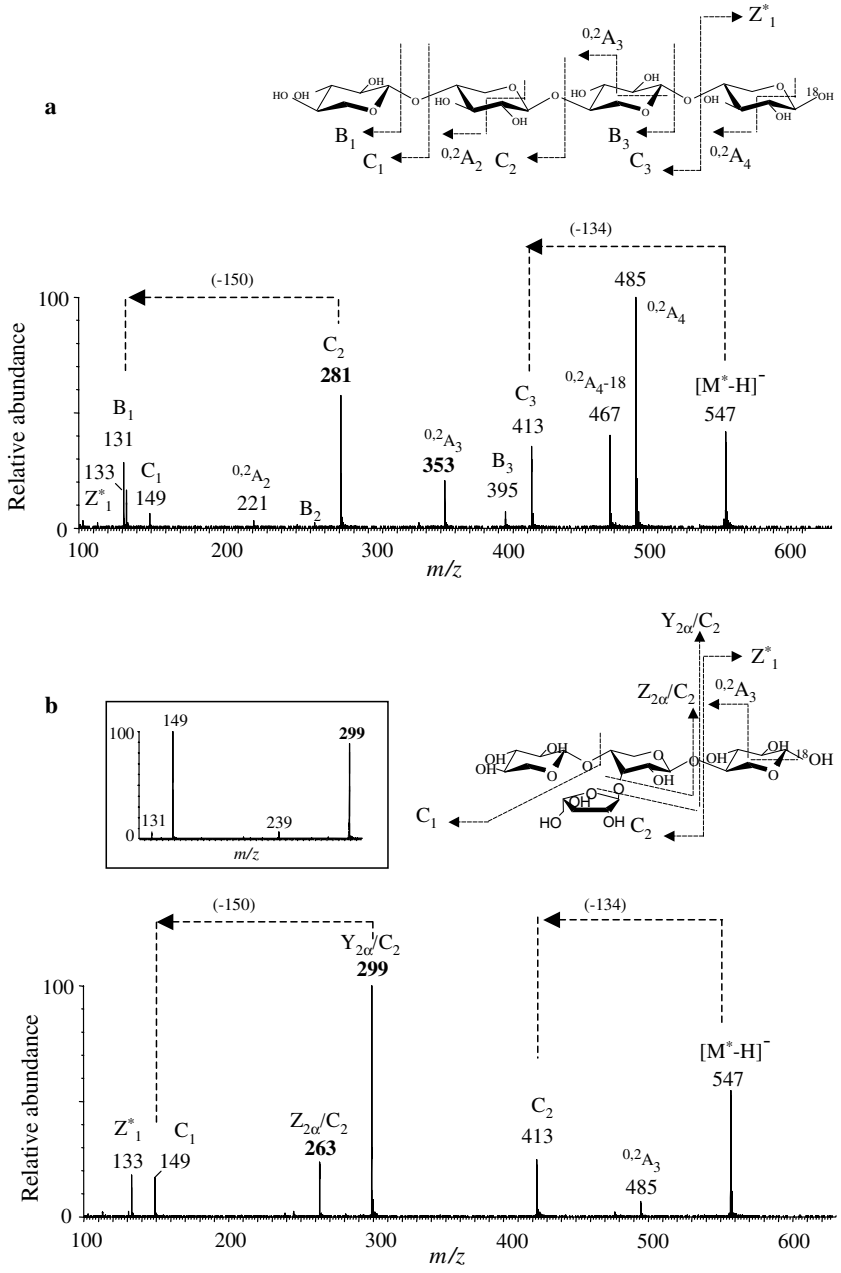


**Figure 2.** Chemical structures and CID mass spectra of the $^{18}$O-labelled $[M^{*}-H]^{-}$ ion from (a) linear xylotetraose, (b) $A1_2X3$ using ESI-Q-TOF at 50% fragmentation level of the $[M^{*}-H]^{-}$ precursor ion; inset: CID mass spectrum of the glycosidic fragment ion at *m/z* 299 after trapping in source. Fragments are identified according to Domon and Costello nomenclature.[48] Asterisks indicate the $^{18}$O-labelled ions.

abundant than the respective one in the CID spectra of mono- and disubstituted AX (DP 4, DP 5 and DP 6, Figs. 2b, 3b and 6a, respectively) obtained using similar collision energies. Due to the $^{18}$O-labelling, this ion was well resolved from the $^{18}$O-labelled $Z_1^{*}$ ion at *m/z* 133.

### 2.3. ESI-CIDMS analysis of monosubstituted arabino-xylo-oligosaccharides

In the following part, xylo-oligosaccharides containing an α-L-arabinofuranosyl residue linked at O-3, in a single or two consecutive or not consecutive xylopyranosyl units in the backbone, are called monosubstituted arabino-xylo-oligosaccharides. Four arabino-xylo-oligosaccharides, namely $A1_2X3$, $A1_3X4$, $A2_{4,3}X5$, and $A2_{5,3}X6$ (Chart 1), isolated from WE-AX by endo-xylanase digestion (*T. viride*) exhibit this pattern of substitution such as the $A1_2X2$ oligosaccharide (provided by Mrs. Helena Rantanen, University of Helsinki, and isolated from rye xylan).

The ESI-Q-TOFMS/MS spectra of the deprotonated $^{18}$O-labelled precursors $[M^{*}-H]^{-}$ of $A1_2X2$, $A1_2X3$ and $A1_3X4$ at *m/z* 415, 547 and 679, respectively, are shown in Figures 1c, 2b and 3b (respectively). In contrast

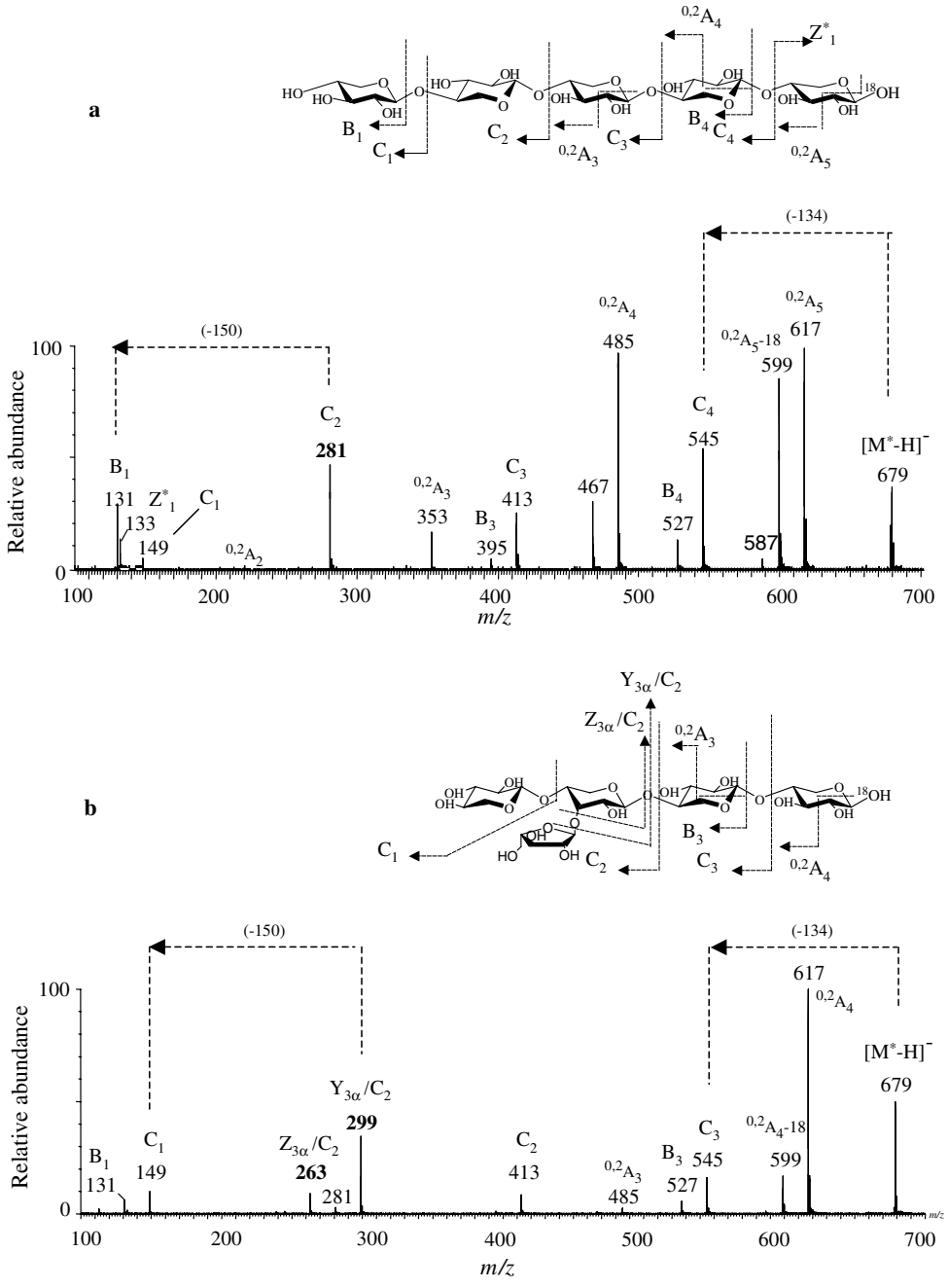


**Figure 3.** Chemical structures and CID mass spectra of the $^{18}$O-labelled $[M^{*}-H]^{-}$ quasi-molecular ion from (a) linear xylopentaose, (b) $A1_3X4$ using ESI-Q-TOF at 50% fragmentation level of the $[M^{*}-H]^{-}$ precursor ion. Fragments are identified according to Domon and Costello nomenclature.[48] Asterisks indicate the $^{18}$O-labelled ions.

with the abundant $^{0,2}A_4$ ion at *m/z* 485 on the CID spectra of linear X4 and X5 (Fig. 2a and 3a, respectively), the $^{0,2}A_3$ ion at *m/z* 485 was a minor ion on the CID spectra of $A1_2X3$ (DP 4) and of $A1_3X4$ (DP 5) (Figs. 2b and 3b, respectively). As CID performed with ESI-ITMS results in similar $MS^2$ profiles (Fig. 4a and d), stabilization of the xylosyl ring by the contiguous monosubstituted xylopyranosyl residue at O-3 might occur. By contrast, the abundance of the $^{0,2}A_4$ ion at *m/z* 617 (Figs. 3b and 4d) could be explained by a smaller stabilizing effect on the terminal free reducing ring in the presence of arabinosyl substituent on the third xylopyranosyl residue. Accordingly, it might be argued that a predominant cross-ring cleavage $^{0,2}A_n$ ion generated from the cleavage of the terminal reducing unit indicates that the first and the second xylosyl residues are not substituted.

Of utmost importance is the predominant glycosidic cleavage ion at *m/z* 299 (Figs. 2b, 3b and 4b), which may result from the combination of both cleavage reactions, namely $C_2$ and $\mathbf{Y}_{2\alpha}$ cleavages in the case of $A1_2X3$,

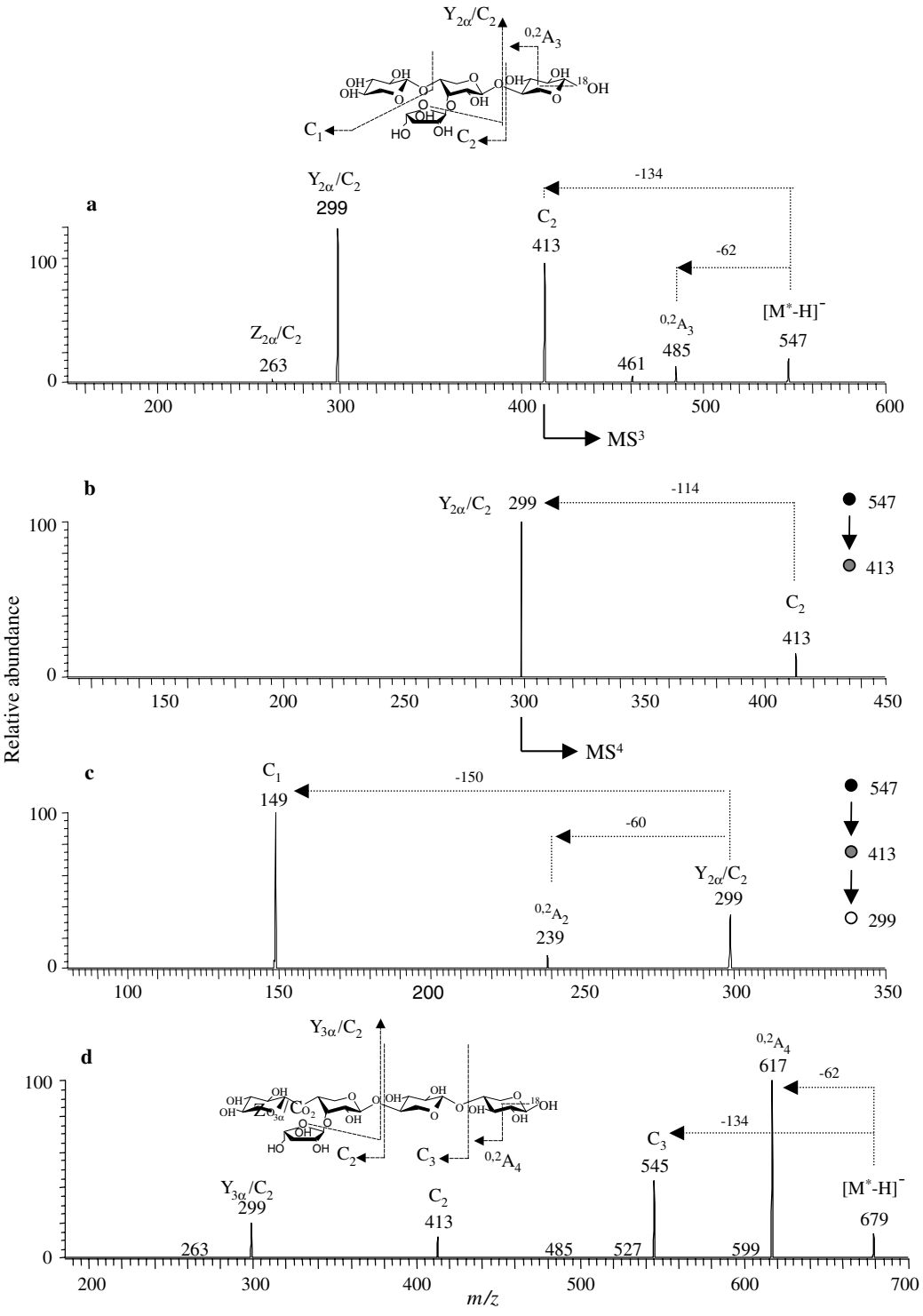


**Figure 4.** Chemical structures and CID mass spectra using ESI-ITMS of the $^{18}$O-labelled $[M^{*}-H]^{-}$ quasi-molecular ion from $A1_2X3$ and $A1_3X4$; (a) $MS^2$ of the parent ion of $A1_2X3$ at *m/z* 547; (b) $MS^3$ experiment (*m/z* 547 > 413); (c) $MS^4$ experiment (*m/z* 547 > 413 > 299); (d) $MS^2$ of the parent ion of $A1_3X4$ at *m/z* 679. The fragments are identified according to Domon and Costello nomenclature.[48]

together with elimination of the arabinosyl substituent at O-3. This monohydrated fragment ion at *m/z* 299 was designated as $\mathbf{Y}_{2\alpha}/C_2$ ion in the case of $A1_2X3$. This fragment was not present in the CID spectrum of the $A1_2X2$ oligosaccharide isolated from rye xylan (Fig. 1c). In other terms, the presence of a major fragment ion at *m/z* 299 is relevant to a penultimate xylosyl residue substituted at O-3 by an arabinosyl unit. The loss of an anhydro-arabinose moiety might be relevant to the furanose form of the arabinosyl ring. To get

better insights into the structure of the fragment ion at *m/z* 299, this ion was selected and fragmented in a MS/MS experiment. In fact, this fragment ion was produced already in the source under the MS conditions used (namely collision energy set to 10 eV) as previously underlined. CID experiment performed on the fragment ion at *m/z* 299 produced the cross-ring fragment ion at *m/z* 239 corresponding to a 60 Da loss and typical of (1→4) xylosyl linkage, and a major glycosidic cleavage $C_1$ ion at *m/z* 149 resulting from a 150 Da loss (see insert in Fig. 2b). Similarly, a $MS^4$ experiment performed on this fragment ion at *m/z* 299 using the ion trap analyser provided the same CID spectrum (Fig. 4c). In both cases, and contrary to linear xylo-oligosaccharides CID spectra, no fragment ions at *m/z* 281 and 263 resulting from water loss were produced. The other important ion was the fragment ion at *m/z* 263 (Figs. 2b and 3b), which may result under its monohydrated form from the combination of both $C_2$ and $\mathbf{Z}_{2\alpha}$ cleavage reactions in the case of $A1_2X3$ and was designated as $\mathbf{Z}_{2\alpha}/C_2$ ion. Both fragment ions at *m/z* 299 and 263, which were not observed in CID experiments with linear xylo-oligosaccharides (Figs. 2a and 3a), may be considered as diagnostic ions for the presence of monosubstitution at the penultimate xylosyl unit. Interestingly, the ratio of their relative intensity was always ~3–5, regardless of the collision energy used in the 10–40 eV range studied, and different from the respective ratio obtained with the disubstituted (on the penultimate xylosyl unit) AX analyzed (see later).

The absence of cross-ring cleavage $^{0,2}A_2$ ions at *m/z* 353 (Figs. 2b and 3b), present on linear isomer CID spectra, is also an important feature of monosubstituted oligosaccharides (Figs. 2a and 3a). $MS^3$ experiment performed on the $C_2$ ion at *m/z* 413 using the ion trap confirmed this result (Fig. 4b). Interestingly, next to the point of branching on the reducing side, the corresponding C-series ions never display the corresponding cross-ring cleavage $^{0,2}$A-series ions, as shown for the $C_3$ ion from $A2_{4,3}X5$ at *m/z* 677 (Fig. 5a), and the $C_4$ ion from $A2_{5,3}X6$ at *m/z* 809 (Fig. 5b). As a consequence, the absence of the $^{0,2}A_2$ ion at *m/z* 221 (Fig. 1d) allows to discriminate $A1_2X2$ from linear xylotriose. In conclusion, the presence of the arabinosyl substituent at O-3 is responsible for the particular fragmentation pathway of monosubstituted xylosyl residues.

Finally, all the MS/MS spectra of the four oligomers monosubstituted at the penultimate xylosyl unit exhibited a noteworthy similar region for ions from *m/z* 149 to *m/z* 413 (Figs. 2b, 3b and 5). Such spectral similarities are structure dependent. In the case of $A2_{5,3}X6$, the cross-ring fragment $^{0,2}A_3$ ion at *m/z* 485 (Fig. 5b), has to be produced from a 60 Da loss from the fourth non-substituted xylosyl unit (from the reducing side). At the opposite, this fragment $^{0,2}A_3$ ion at *m/z* 485 was absent in the MS/MS spectrum of $A2_{4,3}X5$ (Fig. 5a), due to the absence of free xylosyl internal residue. The presence of this cross-ring fragment ion, with its related and abundant glycosidic cleavage ion $C_3$ at *m/z* 545, allowed to discriminate between arabino-xylo-oligosaccharides monosubstituted in non consecutive ($A2_{5,3}X6$) or two consecutive ($A2_{4,3}X5$) xylopyranosyl units in the backbone. The MS/MS spectrum of the $A3_{4,3d}X5$ (DP 8) molecule that contains a mono- and a disubstitution pattern, is discussed in the following section.

### 2.4. ESI-CIDMS analysis of disubstituted arabino-xylo-oligosaccharides

Two arabinosyl residues may be carried at O-2 and O-3 of the same xylosyl unit. Oligomers $A2_{3d}X4$ (DP 6), $A3_{4d,3}X5$ (DP 8) and $A4_{4d,3d}X5$ (DP 9) exhibit such substitution pattern on the penultimate xylosyl unit (Table 1). This structural feature at the non-reducing end was found responsible for common but particular spectral characteristics (Fig. 6). A major fragment ion at *m/z* 263 was always present besides the fragment ion at *m/z* 299 previously described. An intermediary fragment ion at *m/z* 281 was also produced similarly to linear xylo-oligosaccharides. In the case of the highest DP analyzed (DP 9), the major fragment ion at *m/z* 263 was not present when the CID experiment was performed with a collision energy adjusted as to reduce the precursor ion intensity to 50% of its original intensity. However, when the collision energy was increased to reduce the precursor ion intensity to about zero, this diagnostic ion appeared clearly (Fig. 6c). The *m/z* 299/263 peak ratio value was 0.1–0.2 for all the disubstituted (on the penultimate xylosyl residue) AX studied, regardless of the collision energy used in the 10–40 eV range. In other terms, as previously underlined, the value of this ratio may be used to discriminate between arabino-xylo-oligosaccharides mono- or disubstituted on the penultimate xylosyl unit. With this purpose in mind, a mixture of equimolar amounts of two isomeric oligosaccharides, namely $A2_{5,3}X6$ (monosubstituted on the penultimate xylosyl unit) and $A3_{4d,3}X5$ (disubstituted on the penultimate xylosyl unit) was used to carry out MS/MS experiment using a collision energy of 35 eV and measuring the intensity (the ion current on the detector) of both 263 and 299 fragment ions. Intensity was cumulated for 100 spectra and compared to the means of the intensity measured in the same conditions for the respective ion from 100 spectra of each individual isomer. The intensity measured for the fragment ion at *m/z* 263 from the mixture was 85 and fitted well with the respective mean intensity calculated (86). This was also the case for the ion at *m/z* 299 (45 and 50, respectively). As a consequence, the value of the *m/z* 299/263 peak ratio may also be used for detecting co-eluted isomers.

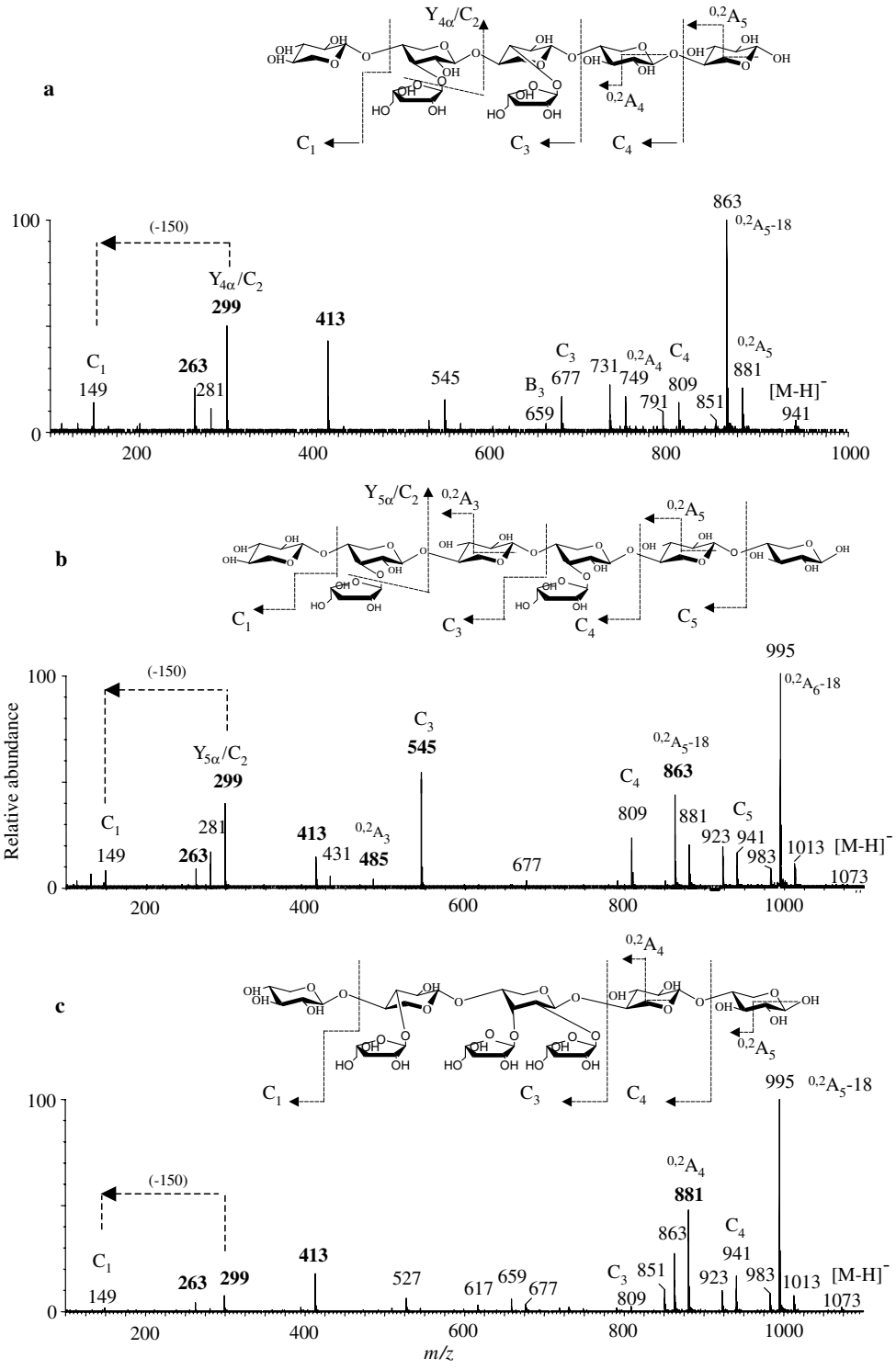


**Figure 5.** Chemical structures and CID mass spectra using ESI-Q-TOF of the $[M-H]^-$ quasi-molecular ion from mono- and disubstituted arabino-xylo-oligosaccharides; (a) $A2_{4,3}X5$; (b) $A2_{5,3}X6$; (c) $A3_{4,3d}X5$, at collision energies required to reduce the abundance of the $[M-H]^-$ precursor ion to 0%. Fragments are identified according to Domon and Costello nomenclature.[48]

Two other important fragment ions were present at *m/z* 395 and 545. The fragment ion at *m/z* 395 might be produced from the fragment ion at *m/z* 545 by loss of 150 Da. In fact, $MS^3$ experiment performed by ESI-ITMS on the fragment ion at *m/z* 545 produced a daughter ion at *m/z* 395 (spectrum not shown). The intensity of the fragment ion at *m/z* 545 was proportional to the collision energy applied. It was low in the case of DP 6 (Fig. 6a), higher for DP 8 (Fig. 6b) and reached a maximum (95% of relative intensity) for

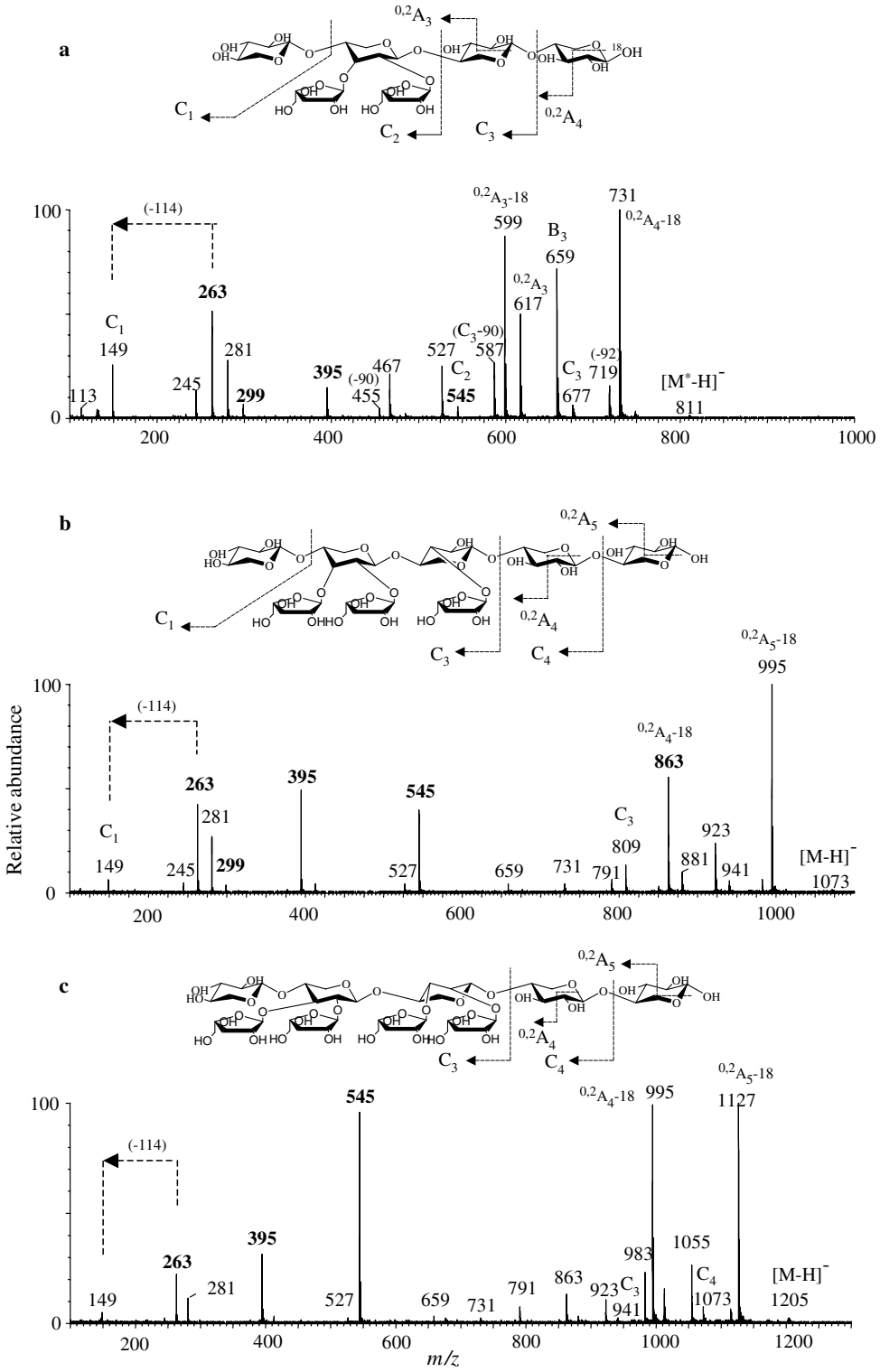


**Figure 6.** Chemical structures and CID mass spectra using ESI-Q-TOF of the $[M-H]^-$ quasi-molecular ion from disubstituted arabino-xylo-oligosaccharides; (a) $^{18}$O-labelled $A2_{3d}X4$, asterisk indicates the $^{18}$O-labelled ion; (b) $A3_{4d,3}X5$; (c) $A4_{4d,3d}X5$, at collision energies required to reduce the abundance of the $[M-H]^-$ precursor ion to 0%. Fragments are identified according to Domon and Costello nomenclature.[48]

DP 9 (Fig. 6c). The MS/MS spectra of these three oligomers disubstituted on the penultimate xylosyl unit exhibited again a remarkable similar region for fragment ions from *m*/*z* 149 to *m*/*z* 395. Note the low intensity of the fragment ion at *m*/*z* 413 (395 + 18), which was always present in MS/MS spectra of monosubstituted arabino-xylo-oligosaccharides (Figs. 2, 3 and 5).

Consider now the MS/MS spectrum of oligomers exhibiting both types of substitution. $A3_{4,3d}X5$ and $A3_{4d,3}X5$ are structural isomers with inversion of their mono- and disubstitution patterns. CID mass spectra of both isomers were recorded at the same collision energy. Interestingly, according to previous observations, both MS/MS spectra were very different, especially the region from $m/z$ 149 to 545 (compare Figs. 5c and 6b). The presence of a monosubstitution at the non-reducing end in the case of the isomer $A3_{4,3d}X5$ was responsible for major fragment ions at $m/z$ 299 and 413 besides traces of ions at $m/z$ 263 and 395 (Fig. 5c). On the contrary, the presence of major fragment ions at $m/z$ 263, 395 and 545 has to be related to the disubstitution at the penultimate xylosyl residue. The presence of two arabinosyl substituents on a xylosyl residue seemed to enhance the production of the $^{0,2}A$ ions generated from the contiguous free xylosyl residue at the reducing end (see high amounts of the $^{0,2}A_3 - 18$ ions at $m/z$ 599 and of $^{0,2}A_4 - 18$ ions at $m/z$ 995 in Fig. 6a and c, respectively). At the opposite, the glycosidic cleavage $C_i$ ions next to the branched point (on the reducing side) were produced in low abundance. Indeed, the glycosidic cleavage $C_2$ and $C_3$ ions at $m/z$ 545 and 941 were scarcely abundant on the CID spectra of $A2_{3d}X4$ and of $A4_{4d,3d}X5$ (Fig. 6a and c respectively).

### 2.5. Conclusions

The main features of CID mass spectra related to differences in the pattern of substitution of arabino-xylo-oligosaccharides have been established. The eight mono- and disubstituted xylo-oligosaccharides examined were released by enzymatic degradation of wheat WE-AX by an endoxylanase from *T. viride*. Their previous characterization by $^1$H NMR spectroscopy has revealed substitution of β-(1→4) linked xylosyl residues by arabinose at O-3 and O-2 on a single or on two contiguous xylosyl residues. This knowledge, combined with the labelling of the reducing end using $H_2{}^{18}O$, was particularly useful for the interpretation of CID MS spectra obtained by ESI-Q-TOF namely to ascertain that the fragmentation under CID performed in negative-ion mode always proceeds from the reducing end. CID-MS analysis also provided evidences for the presence of two free xylosyl residues at the reducing side and of one free xylosyl residue at the non-reducing side. A mono- or a disubstitution of the penultimate xylosyl residue (from the non-reducing side) was also responsible for characteristic CID spectra. ESI-Q-TOF technology was particularly efficient for the structural analysis of oligomers of high polymerization degree, up to DP 9, namely for the differentiation of DP 8 isomers.

It is generally considered that derivatization of oligosaccharides by permethylation remains a prerequisite to deliver valuable structural information and that the conversion of oligosaccharides to hydrophobic derivatives enhances signal intensity regardless of the ionization technique used.[52] However, the amount of material required by this additional derivatization step is superior to the 0.5–1 μg of underivatized oligosaccharide used here per sample. Finally, compared with ESI-Q-TOF used in positive-ion mode, which only delivers sequence information,[40,41,51] the results shown here indicate that ESI-Q-TOF used in negative-ion mode is a relevant technique for the structural analysis of underivatized branched oligosaccharides generated from arabinoxylans.

## 3. Experimental

### 3.1. Materials

Eight arabino-xylo-oligosaccharides with substitution of the β-(1→4)-linked xylose framework by arabinose at O-3 or O-2 and O-3 on a single or on two contiguous xylosyl residues, were isolated and purified from the digestion of WE-AX by a *T. viride* endoxylanase (Chart 1). Their structure was determined by $^1$H NMR spectroscopy as previously described.[47] $A1_2X2$ oligosaccharide was kindly provided by Mrs. Helena Rantanen (University of Helsinki) and was isolated and purified from enzymatic hydrolysis of rye xylan by an *endo*-β-D-xylanase (Novozymes). Its chemical structure was determined by $^1$H NMR spectroscopy and MALDI-TOFMS. Linear xylo-oligosaccharides of DP 3, 4, 5 and 6, named X3, X4, X5 and X6, respectively, were purchased from Megazyme (Bray, Ireland). $H_2{}^{18}O$ (95 at % $^{18}O$) was purchased from Sigma–Aldrich (St. Louis, MO, USA).

### 3.2. $^{18}$O-Labelling

The reducing end of oligosaccharides was labelled with $^{18}O$ by adding about 20 μL of $H_2{}^{18}O$ to 20–40 μg of freeze-dried sample. The samples were left at least 72 h at ambient temperature in a desiccator. The $^{18}O$-labelling allows to differentiate glycosidic cleavage ions, especially $B_i$ from $Z_j$ ions and $C_i$ from $Y_j$ ions. $^{18}O$-Labelled quasi-molecular and $Z_j$ ions are represented as $M^*$ and $Z_j{}^*$, respectively. The ions of the B- and C-series are not labelled as they do not contain the labelled anomeric hydroxyl group. Their respective complementary ions, $Y_j{}^*$ and $Z_j{}^*$ ions, which contain the labelled $^{18}O$ from the hydroxyl of the reducing end have a mass increment of 2 Da.

### 3.3. ESI-Q-TOF mass spectrometry

Analysis by electrospray ionization quadrupole time-of-flight mass spectrometry of $^{18}O$-labelled linear xylo-oligosaccharides and of purified arabino-xylo-oligosaccharides was performed on a Micromass Q-TOF Ultima Global mass spectrometer (Micromass Ltd.,

Manchester, UK). MS and MS/MS spectra were acquired in negative-ion mode. Desalted $^{18}O$-labelled arabino-xylo-oligosaccharides were diluted in 1:1 MeOH–water in order to obtain a final concentration ~1–3 μg/mL. Sample solns were introduced at 3 μL/min using an ESI-probe. The ion source was set to 80 °C and the desolvation temperature to 120 °C. Nitrogen was used as drying gas. The needle voltage was maintained at 3 kV and the cone voltage was adjusted at 100 V. The scan time and the interscan delay were set to 1 and 0.5 s, respectively. For CID experiments, argon was used as the collision gas. The precursor ion was selected in the first quadrupole, and fragmented in the hexapole collision cell. Collision energies were adjusted in order to get a relative intensity of the parent ion of 50% or ~0%. For comparative studies of structural isomers (AX with the same DP) the same collision energy, in the 10–40 eV range, was used for the MS/MS fragmentation. MS/MS spectra were recorded for 2 min in order to maximize the signal/noise ratio.

### 3.4. ESI-IT mass spectrometry

All the $^{18}O$-labelled oligosaccharides were also analyzed by negative ESI-ITMS$^n$ using a LCQ Advantage ion trap mass spectrometer (Thermo Electron, USA). Desalted $^{18}O$-labelled arabino-xylo-oligosaccharides were diluted in 1:1 MeOH–water to favour the spray formation into the electrospray source and to obtain a final concentration of ~50 μg/mL. Sample introduction was performed at a flow-rate of 2.5 μL/min. Nitrogen was used as sheath gas (20 arbitrary units). The MS analyses were carried out using automatic gain control conditions, with a typical needle voltage of 4 kV and a heated capillary temperature of 200 °C. For MS$^n$ experiments, the various parameters (collision energy, activation time, ...) were adjusted for each sample in order to optimize the signal and get maximal structural information from the selected ion. As the exchange kinetic is low, no significant back-exchange $^{16}O$ was observed during the analysis duration (about 15 min). A total of 30–50 scans were summed for spectra acquisition.

## Acknowledgements

The authors thank Mrs. Helena Rantanen from the Department of Applied Chemistry and Microbiology, University of Helsinki (Finland), for the gift of the $A1_2X2$ sample and Dr. Olivier Laprévote from ICSN, CNRS, F-91198 Gif-sur-Yvette (France) for helpful discussion. J. J. Ordaz-Ortiz is grateful to the Consejo Nacional de Ciencia y Tecnología-México (CONACyT) for financial support.

## References

1. Izydorczyk, M. S.; Biliaderis, C. G. *Carbohydr. Polym.* **1995**, *28*, 33–48.
2. Gruppen, H.; Kormelink, F. J. M.; Voragen, A. G. J. *J. Cereal Sci.* **1993**, *18*, 129–143.
3. Ordaz-Ortiz, J. J.; Saulnier, L. *J. Cereal Sci.* **2005**, *42*, 119–125.
4. Hoffmann, R. A.; Leeflang, B. R.; Debarse, M. M. J.; Kamerling, J. P.; Vliegenthart, J. F. G. *Carbohydr. Res.* **1991**, *221*, 63–81.
5. Hoffmann, R. A.; Kamerling, J. P.; Vliegenthart, J. F. G. *Carbohydr. Res.* **1992**, *226*, 303–311.
6. Hoffmann, R. A.; Geijtenbeek, T.; Kamerling, J. P.; Vliegenthart, J. F. G. *Carbohydr. Res.* **1992**, *223*, 19–44.
7. Gruppen, H.; Hoffmann, R. A.; Kormelink, F. J. M.; Voragen, A. G. J.; Kamerling, J. P.; Vliegenthart, J. F. G. *Carbohydr. Res.* **1992**, *233*, 45–64.
8. Kormelink, F. J. M.; Hoffmann, R. A.; Gruppen, H.; Voragen, A. G. J.; Kamerling, J. P.; Vliegenthart, J. F. G. *Carbohydr. Res.* **1993**, *249*, 369–382.
9. Viëtor, R. J.; Hoffmann, R. A.; Angelino, S. A. G. F.; Voragen, A. G. J.; Kamerling, J. P.; Vliegenthart, J. F. G. *Carbohydr. Res.* **1994**, *254*, 245–255.
10. Debyser, W.; Schooneveld-Bergmans, M. E. F.; Derdelinckx, G.; Grobet, P. J.; Delcour, J. A. *J. Agric. Food Chem.* **1997**, *45*, 2914–2918.
11. Schooneveld-Bergmans, M. E. F.; Beldman, G.; Voragen, A. G. J. *J. Cereal Sci.* **1999**, *29*, 63–75.
12. Broberg, A.; Thomsen, K. K.; Duus, J. Ø. *Carbohydr. Res.* **2000**, *328*, 375–382.
13. Ferré, H.; Broberg, A.; Duus, J. Ø.; Thomsen, K. K. *Eur. J. Biochem.* **2000**, *267*, 6633–6641.
14. Garozzo, D.; Giuffrida, M.; Impallomeni, G.; Ballistreri, A.; Montaudo, G. *Anal. Chem.* **1990**, *62*, 279–286.
15. Zhou, Z.; Ogden, S.; Leary, J. A. *J. Org. Chem.* **1990**, *55*, 5444–5446.
16. Hofmeister, G. E.; Zhou, Z.; Leary, J. A. *J. Am. Chem. Soc.* **1991**, *113*, 5964–5970.
17. Asam, M. R.; Glish, G. L. *J. Am. Soc. Mass Spectrom.* **1997**, *8*, 987–995.
18. Quéméner, B.; Ralet, M.-C. *J. Mass Spectrom.* **2004**, *39*, 1153–1160.
19. Harvey, D. J. *J. Mass Spectrom.* **2000**, *35*, 1178–1190.
20. Harvey, D. J. *J. Am. Soc. Mass Spectrom.* **2001**, *12*, 926–937.
21. Korner, R.; Limberg, G.; Christensen, T. M.; Mikkelsen, J. D.; Roepstorff, P. *Anal. Chem.* **1999**, *71*, 1421–1427.
22. Mutenda, K. E.; Korner, R.; Christensen, T. M.; Mikkelsen, J. D.; Roepstorff, P. *Carbohydr. Res.* **2002**, *337*, 1217–1227.
23. Quéméner, B.; Désiré, C.; Debrauwer, L.; Negroni, L.; Lahaye, M. *Eur. J. Mass Spectrom.* **2003**, *9*, 45–60.
24. Quéméner, B.; Cabrera Pino, J.-C.; Ralet, M.-C.; Bonnin, E.; Thibault, J.-F. *J. Mass Spectrom.* **2003**, *38*, 641–648.
25. Levigne, S.; Ralet, M.-C.; Quéméner, B.; Thibault, J.-F. *Carbohydr. Res.* **2004**, *339*, 2315–2319.
26. Ralet, M.-C.; Cabrera Pino, J.-C.; Bonnin, E.; Quéméner, B.; Hellin, P.; Thibault, J.-F. *Phytochemistry* **2005**, *66*, 1832–1843.
27. Reinhold, V. N.; Reinhold, B. B.; Costello, C. E. *Anal. Chem.* **1995**, *67*, 1772–1784.
28. Weiskopf, A. S.; Vouros, P.; Harvey, D. J. *Rapid Commun. Mass Spectrom.* **1997**, *11*, 1493–1504.

29. Viseux, N.; de Hoffmann, E.; Domon, B. *Anal. Chem.* **1997**, *69*, 3193–3198.
30. Yoshino, K.; Takao, T.; Murata, H.; Shimonishi, Y. *Anal. Chem.* **1995**, *67*, 4028–4031.
31. Ahn, Y. H.; Yoo, J. S. *Rapid Commun. Mass Spectrom.* **1988**, *12*, 2011–2015.
32. Li, D. T.; Her, G. R. *J. Mass Spectrom.* **1988**, *33*, 644–652.
33. Charlwood, J.; Langridge, J.; Tolson, D.; Birrel, H.; Camilleri, P. *Rapid Commun. Mass Spectrom.* **1999**, *13*, 107–112.
34. Shen, X.; Perreault, H. *J. Mass Spectrom.* **1988**, *34*, 502–510.
35. Lemoine, J.; Fournet, B.; Despeyroux, D.; Jennings, K. R.; Rosenberg, R.; de Hoffmann, E. *J. Am. Soc. Mass Spectrom.* **1993**, *4*, 197–203.
36. Fura, A.; Leary, J. A. *Anal. Chem.* **1993**, *65*, 2805–2811.
37. Staempfli, A.; Zhou, Z.; Leary, J. A. *J. Org. Chem.* **1992**, *57*, 3594–3599.
38. Cancilla, M. T.; Penn, S. G.; Carroll, J. A.; Lebrilla, C. B. *J. Am. Chem. Soc.* **1996**, *118*, 6736–6745.
39. König, S.; Leary, J. A. *J. Am. Soc. Mass Spectrom.* **1998**, *9*, 1125–1134.
40. Matamoros-Fernández, L. E.; Obel, N.; Scheller, H. V.; Roepstorff, P. *J. Mass Spectrom.* **2003**, *38*, 427–437.
41. Matamoros-Fernández, L. E.; Obel, N.; Scheller, H. V.; Roepstorff, P. *Carbohydr. Res.* **2004**, *339*, 655–664.
42. Chai, W.; Piskarev, V.; Lawson, A. M. *Anal. Chem.* **2001**, *73*, 651–657.
43. Chai, W.; Piskarev, V.; Lawson, A. M. *J. Am. Soc. Mass Spectrom.* **2002**, *13*, 670–679.
44. Quéméner, B.; Désiré, C.; Debrauwer, L.; Rathahao, E. *J. Chromatogr., A* **2003**, *984*, 185–194.
45. Vakhrushev, S. Y.; Zamfir, A.; Katalini'c, J. P. *J. Am. Soc. Mass Spectrom.* **2004**, *15*, 1863–1868.
46. Carroll, J. A.; Ngoka, L.; Beggs, C. G.; Lebrilla, C. B. *Anal. Chem.* **1993**, *65*, 1582–1587.
47. Ordaz-Ortiz, J. J.; Guillon, F.; Tranquet, O.; Dervilly-Pinel, G.; Tran, V.; Saulnier, L. *Carbohydr. Polym.* **2004**, *57*, 425–433.
48. Domon, B.; Costello, C. E. *Glycoconjugate J.* **1998**, *5*, 397–409.
49. Levigne, S.; Ralet, M.-C.; Quéméner, B.; Pollet, B. M.-L.; Lapierre, C.; Thibault, J.-F. *Plant Physiol.* **2004**, *134*, 1173–1180.
50. Mulroney, B.; Peel, J. B.; Traeger, J. C. *J. Mass Spectrom.* **1999**, *34*, 856–871.
51. Reis, A.; Coimbra, M. A.; Domingues, P.; Ferrer-Correira, A. J.; Domingues, M. R. M. *Carbohydr. Polym.* **2004**, *55*, 401–409.
52. Viseux, N.; de Hoffmann, E.; Domon, B. *Anal. Chem.* **1998**, *70*, 4951–4959.